RSC Applied Polymers

ROYAL SOCIETY OF CHEMISTRY

PAPER

View Article Online
View Journal | View Issue



Check for updates

Cite this: *RSC Appl. Polym.*, 2024, **2**, 461

# Chitosan–saccharide conjugates for eradication of *Pseudomonas aeruginosa* biofilms†

Priyanka Sahariah, *[a] Francesco Papi, [b] Koi L. Merz,[b] Olafur E. Sigurjonsson, [c] Rikke Loiuse Meyer [d,e] and Cristina Nativi [b]

Received 29th November 2023,
Accepted 27th February 2024

DOI: 10.1039/d3lp00263b

rsc.li/rscapplpolym

The problem of antibiotic resistance has raised serious concerns globally and hence the development of new materials which can combat these drug-resistant strains has gained a great deal of attention. Herein, we report the use of a biocompatible material, chitosan, as a scaffold to graft saccharides which can specifically target *Pseudomonas aeruginosa*. We realized this by synthesizing *N*-functionalized chitosan conjugates by coupling chitosan to fucose and galactose moieties which intercept *Pseudomonas aeruginosa* lectins and target the bacterial biofilms. A series of six conjugates containing similar proportions of cationic and sugar moieties were synthesized by direct modification of the chitosan backbone using a method that is highly efficient and reproducible. The conjugates showed a bactericidal effect against both Gram positive and Gram negative bacterial strains. An investigation into the antibiofilm activity of the conjugates revealed the optimum combination of the type and positioning of the functionalities that were highly effective in eradicating *Pseudomonas aeruginosa* biofilms. 2D and 3D imaging of the conjugate-treated biofilms using confocal laser scanning microscopy (CLSM) allowed us to determine that the conjugates not only acted on the surface but also dispersed into deep layers of the biofilm. Interaction between the conjugates and individual bacterial cells in the biofilm was further confirmed by fluorescence labelling of the conjugates and imaging by CLSM.

## Introduction

Antimicrobial resistance has emerged as a global concern with the currently available antibiotics becoming ineffective in controlling infections. Among the WHO priority pathogens, *Pseudomonas aeruginosa* (*P. aeruginosa*) has been identified as one of the most life-threating bacteria and has been prioritized for research and development of new antibiotics.[1,2] *P. aeruginosa*, a Gram-negative bacterium, causes severe infections in immunocompromised hosts leading to clinically persistent infections such as cystic fibrosis, urinary tract infections, and burn infections.[3] The antibiotic resistance in *P. aeruginosa* is attributed to multiple mechanisms and a variety of virulence factors, of which its ability to form biofilms is an important mechanism by which it can also resist host defenses.[4] Biofilms of *P. aeruginosa* are formed due to the secretion of extracellular polymeric substances which adhere to the bacterial cells forming a matrix. The growing microbial cells embedded in this matrix become less susceptible to antibiotics or host defence systems than the cells in the planktonic form.[5] Moreover, biofilm formation is an adaptive mechanism, so the microbial cells can regain antibiotic susceptibility once they lose biofilm protection.[6] Hence, developing molecules that can penetrate the biofilm and interact with the microbial cells embedded in the matrix is crutial for displaying activity against *P. aeruginosa*.

Biofilm formation in *P. aeruginosa* infections is mediated by galactose-specific lectin A (LecA, PA-IL) and fucose-specific lectin B (LecB, PA-IIL). Indeed, the effect of simple derivatives of galactose and fucose on inhibiting the bacterium from producing a biofilm was demonstrated by *in vitro* and *in vivo* studies. α-*C*-Fucosyl and β-*O*-aryl galactosyl derivatives grafted onto peptide dendrimers showed remarkably increased affinity for LecB and LecA, respectively, up to 100 times and up to 4000 times greater than that of simple carbohydrates, maintaining biofilm inhibition properties.[7] Recent studies have also shown the efficiency of other glycopolymers in binding LecA and LecB and inhibiting or disrupting *P. aeruginosa* biofilm formation.[8]

Chitosan is a biocompatible linear polymer containing β(1 → 4) linked residues of *N*-acetyl-2 amino-2-deoxy-D-glucose

[a]*Department of Life and Environmental Sciences, Biomedical Centre, University of Iceland, 101 Reykjavik, Iceland. E-mail: prs@chemrsc.org*
[b]*Department of Chemistry, University of Florence, Sesto F.no, Florence, Italy*
[c]*The REModeL Lab, The Blood Bank, Landspitali University Hospital, Snorrabraut 60, 105 Reykjavik, Iceland*
[d]*iNANO, Aarhus University, Gustav Weids Vej 14, 8000 Aarhus C, Denmark*
[e]*Department of Bioscience, Aarhus University, Ny Munkegade 114, 8000 Aarhus C, Denmark*

† Electronic supplementary information (ESI) available. See DOI: https://doi.org/10.1039/d3lp00263b

(glucosamine, GlcN) and 2-amino-2-deoxy-D-glucose (*N*-acetylglucosamine, GlcNAc) residues. Chitosan is endowed with many biological and technological properties such as mucoadhesive, anti-inflammatory, antioxidant, antimicrobial, antifungal, antitumor and wound healing properties.[9] In recent years, chitosan has attracted huge attention due to its antimicrobial properties as evidenced by the significant number of publications. An emerging area is the chemical manipulation of the chitosan backbone to modify the free –OH or $-NH_2$ group or to link various biomolecules, all with the intention of enhancing its antimicrobial properties.[10] Synthesis of various chitosan conjugates such as chitosan–peptide, chitosan–porphyrin, chitosan–PEG, polyphenol–chitosan, and chitosan–cinnamic acid derivatives has been reported for enhancing the aqueous solubility and antimicrobial activity of the native polymer.[11,12] A series of chitosan–antimicrobial peptide (chitosan–AMP) conjugates not only displayed enhanced antimicrobial activity towards Gram-positive and Gram-negative bacteria, but significantly reduced the overall toxicity of the AMPs.[13] Chitosan peptide conjugates have also gained interest in the design of antimicrobial coatings, such as the ε-polylysine–chitosan conjugate against *Staphylococcus epidermidis*, *Escherichia coli* (*E. coli*), *Staphylococcus aureus* (*S. aureus*), *Bacillus subtilis* and beer yeast[14,15] and peptidoglycan mimetic-chitosan against *E. coli*.[16] Recently, studies have shown the efficiency of chitosan-based conjugates against bacterial biofilms. Conjugation of aminoglycoside antibiotics such as streptomycin to chitosan, damaged established biofilms, and inhibited biofilm formation in Gram positive bacteria *Listeria monocytogenes*,[17] while DNase I supplemented with chitosan (CS) linked with CAZ (CS/CAZ) significantly eradicated *Burkholderia pseudomallei* biofilm cells.[18]

Hence, the aim of this study was to rely on the ability of aryl-*O*-galactoside and *C*-fucosides to intercept bacterial LecA and LecB and form sugar–chitosan conjugates to treat and disrupt established biofilms of *P. aeruginosa*. With this aim, we prepared glycosides **S1** and **S2** which present a five-carbon linker with a terminal carboxylic group (see Scheme 1 and the ESI†). By introducing a specific ratio of the two glycosides on natural chitosan, we aimed to synthesize a series of conjugates and compare their ability to interact with *P. aeruginosa* biofilms. Moreover, to observe the synergistic effect of antimicrobial cationic functionalities and the two lectins' ligands, we also introduced **S1** and **S2** moieties on two cationic chitosan derivatives.

The cationic modifications on chitosan consist in the introduction of the trimethylammoniumyl group either directly at the free amino group or using spacers. We introduced the cationic groups and the sugar moiety each at ~25% to have at least 50% of the free amino groups on the chitosan backbone. By utilizing the mesylate salt of chitosan, we developed a synthetic method for direct modification of the free amino group in chitosan as well as for linking the glycosyl moieties through amide bond formation (see Scheme 1). Avoiding the use of protective groups, we reduced the complexity of the synthesis and produced a series of six sugar–chitosan conjugates with excellent reproducibility. Antibacterial assessment of the conjugates against both Gram-positive and Gram-negative bacteria allowed us to determine the spectrum of their antibacterial activity. We then utilized the conjugates specifically to interact and eradicate preformed biofilms of *P. aeruginosa*. Morphological changes in *P. aeruginosa* biofilms were confirmed visually by confocal laser scanning microscopy (CLSM) imaging of the polymer-treated biofilms. Furthermore, we confirmed that the conjugates interact with *P. aeruginosa* cells by visualizing the effect of the conjugates on *P. aeruginosa* cells by fluorescence staining and CLSM.

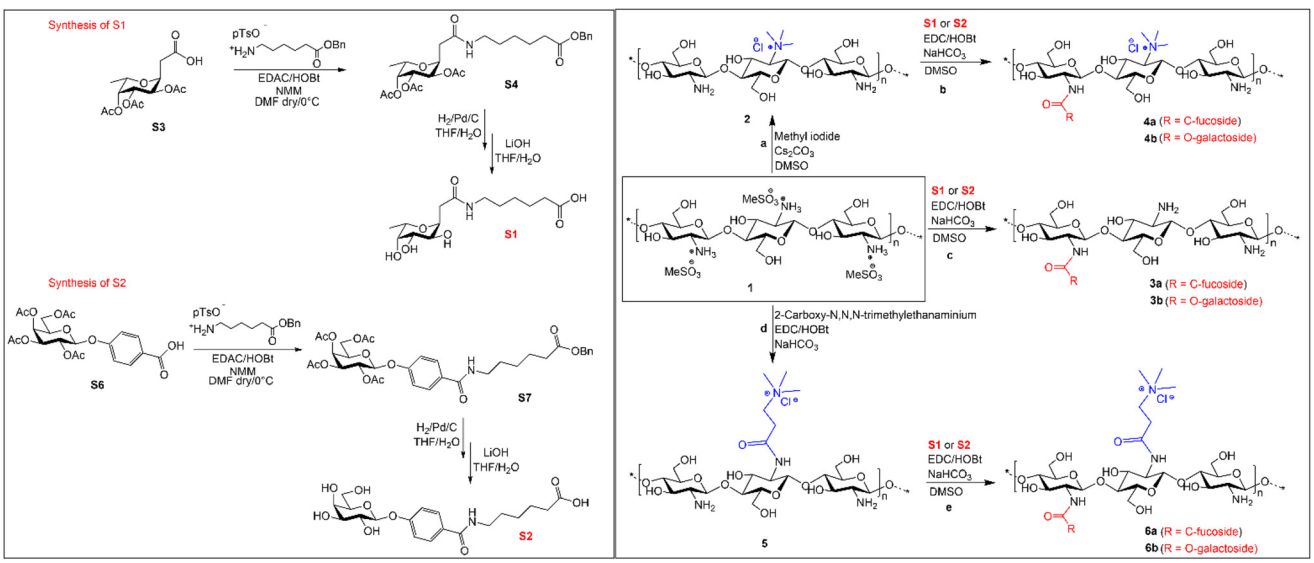


**Scheme 1** Synthetic scheme for the synthesis of *C*-fucoside **S1**, *O*-galactoside **S2** and sugar–chitosan conjugates **6a** and **6b** from the chitosan mesylate salt. (Details of **S1** and **S2** synthesis are provided in the ESI.†)

# Experimental

## Materials and methods

Chitoceutical Chitosan 95/10 (24701) was purchased from Heppe Medical Chitosan GmbH, Halle, Germany. The degree of acetylation of chitosan was calculated to be 5% by $^1$H-NMR spectroscopy. The average molecular weight ($M_w$) and dispersity ($D$) of the chitosan were determined to be 27 kDa and 2.1, respectively, by gel permeation chromatography. Gram positive bacteria *S. aureus* (DSM 20231) and Gram-negative bacteria *E. coli* (ATCC 25922) and *P. aeruginosa* (PA01 DSM19880) were obtained from DSMZ – German collection of Microorganisms and Cell cultures Gmbh. All other chemicals were purchased from Merck. Silica gel flash column chromatography purifications were performed using Geduran® Si 60 (0.040–0.063 mm). TLC analyses were performed on glass Merck silica gel 60 F254 plates. $^1$H NMR, $^{13}$C NMR and 2D-NMR spectra were recorded on a 500 MHz Bruker AVANCE II at 298 K.

## Synthetic procedures

**Chitosan mesylate salt 1.** Chitosan mesylate salt (1.5 g) was prepared according to a previously published procedure.[19] The resulting light brown solid was freely soluble in water (at pH = 7) and dimethyl formamide (DMF) at a concentration of 50 mg mL$^{-1}$.

Yield: 2.31 g (97.1%). $^1$H NMR (500 MHz, $D_2O$): $\delta$ 2.84 (s, $CH_3$), 3.21 (s, H-2), 3.78–3.96 (m, H-3, H-4, H-5, H-6), 4.90 (H-1, partially overlapped by the water peak) ppm.

**General procedure for the synthesis of sugar–chitosan (CS-S1, 4a, and CS-S2, 4b) conjugates.** Chitosan mesylate salt (0.5 g, 1 eq., 2.31 mmol) was dissolved in DMF (10 mL) under stirring. **S1** or **S2** (0.5 eq., 1.15 mmol) was dissolved in DMF (5 mL) and EDC (0.5 eq., 1.15 mmol) and HOBt (0.5 eq., 1.15 mmol) were added followed by stirring for 1 h at 25 °C. The solution of chitosan mesylate salt was then added to the reaction mixture along with sodium bicarbonate ($NaHCO_3$) (0.39 g, 2 eq., 4.63 mmol). The reaction was stirred at 55 °C for 18 h. The reaction mixture was diluted with ice-cold water and dialysed against water for 2 days, ion-exchanged against 10% sodium chloride solution and re-dialysed for 2 days. The purified solution was lyophilized to get a light-yellow solid as the product. **CS-S1**: yield: 0.72 g (96%). $^1$H NMR (500 MHz, $D_2O$): $\delta$ 1.00 (9), 1.19 (5), 1.37–1.45 (4,6), 1.90 (3), 2.16–2.41 (8), 2.72 (7), 3.03–3.77 (glucose + glucosamine unit), 4.25–4.44 (H-1) ppm. **CS-S2**: yield: 0.81 g (94%). $^1$H NMR (500 MHz, $D_2O$): $\delta$ 1.42 (5), 1.65 (4,6), 2.08 (N-Ac), 2.41 (3), 3.20 (7), 3.38–3.93 (glucose + glucosamine unit), 4.88 (H-1), 6.98–7.22 (8), 7.68–7.75 (9) ppm.

***N*,*N*,*N*-Trimethyl chitosan (TMC), 2.** Chitosan mesylate salt (0.5 g, 1 eq., 2.31 mmol) was dissolved in DMSO (10 mL) and cesium carbonate ($Cs_2CO_3$) (1.52 g, 1 eq., 2.31 mmol) was added to the solution under stirring. After 0.5 h, methyl iodide (MeI) (0.52 mL, 0.5 eq., 1.15 mmol) was added to the reaction mixture and the reaction was heated to 55 °C for 18 h. The reaction mixture was diluted with ice-cold water and dialysed against water for 2 days, ion-exchanged against 10% sodium chloride solution and re-dialysed for 2 days. The purified solution was lyophilized to get a white solid as the product, **TMC**. Yield: 0.58 g (92.1%). $^1$H NMR (500 MHz, $D_2O$): $\delta$ 3.18 [N$(CH_3)_3$], 3.77–3.91 (H-2–H-6, glucosamine unit), 4.79 (H-1 merged with the $D_2O$ peak) ppm.

**General procedure for the synthesis of TMC–sugar conjugates (TMC-S1, 3a, and TMC-S2, 3b).** TMC (0.5 g, 1 eq., 2.42 mmol) was dissolved in DMF (10 mL) under stirring. **S1** or **S2** (0.5 eq., 1.21 mmol) was dissolved in DMF and EDC (0.5 eq., 1.21 mmol) and HOBt (0.5 eq., 1.21 mmol) were added followed by stirring for 1 h at 25 °C. The solution of TMC was then added to the reaction mixture along with $NaHCO_3$ (0.39 g, 4.63 mmol). The reaction was stirred at 55 °C for 18 h. The reaction mixture was diluted with ice-cold water and dialysed against water for 2 days, ion-exchanged against 10% sodium chloride solution and re-dialysed for 2 days. The purified solution was lyophilized to get a light-yellow solid as the product. **TMC-S1**: yield: 0.67 g (94%). $^1$H NMR (500 MHz, $D_2O$): $\delta$ 1.14 (9), 1.32 (5), 1.50 (4), 1.59 (6), 2.03 (N-Ac), 2.36 (3), 2.53–2.63 (8), 2.86 (7), 3.13 [N$(CH_3)_3$], 3.72–4.38 (glucose + glucosamine unit), 4.79 (H-1 merged with $D_2O$) ppm. **TMC-S2**: yield: 0.71 g (87.7%). $^1$H NMR (500 MHz, $D_2O$): $\delta$ 1.38 (5), 1.63 (4,6), 2.07 (N-Ac), 2.19 (3), 2.88–3.16 (7), 3.36 [N$(CH_3)_3$], 3.66–4.01 (glucose + glucosamine unit), 4.61–5.14 (H-1), 7.20 (8), 7.74 (9) ppm.

***N*,*N*,*N*-Trimethylaminepropanoic acid.** 3-Bromopropanoic acid (2 g, 1 eq., 13.1 mmol) was dissolved in DCM under a $N_2$ atmosphere. Excess $Me_3N$ (4.2 molar in EtOH) (10 mL) was added and the resulting mixture was stirred for 24 h at 25 °C. The reaction mixture was concentrated *in vacuo* and triturated with DCM to get the pure product. Yield: 1.5 g (90.4%). $^1$H NMR (500 MHz, $D_2O$): $\delta$ 2.85 (N–$CH_2$–), 3.15 [N$(CH_3)_3$], 3.64 (CO–$CH_2$–) ppm.

***N*,*N*,*N*-Trimethyl-*N*-propanoyl-chitosan (TPC), 5.** Chitosan mesylate salt (0.5 g, 1 eq., 2.31 mmol) was dissolved in DMF (10 mL) under stirring. *N*,*N*,*N*-trimethylaminepropanoic acid (0.35 g, 0.5 eq., 1.15 mmol), EDC (0.22 g, 0.5 eq., 1.15 mmol) and HOBt (0.16 g, 0.5 eq., 1.15 mmol) were stirred in DMF for 1 h at 25 °C and finally added to the solution of chitosan mesylate salt. Sodium bicarbonate ($NaHCO_3$) (0.39 g, 2 eq., 4.63 mmol) was added to the reaction mixture and the reaction was stirred at 55 °C for 8 h. The reaction mixture was diluted with ice-cold water and dialysed against water for 2 days, ion-exchanged against 10% sodium chloride solution and re-dialysed for 2 days. The purified solution was lyophilized to get a light-yellow solid as the product, TPC. Yield: 0.72 g (84.7%). $^1$H NMR (500 MHz, $D_2O$): $\delta$ 1.81 (N-Ac), 2.61 (–$CH_2$–N), 2.81 [N$(CH_3)_3$], 2.94 (CO–$CH_2$–), 3.07–3.14 (H2), 3.52–3.98 (H-3–H-6, glucosamine unit), 4.64 (H-1) ppm.

**General procedure for the synthesis of TPC–sugar conjugates (TPC-S1, 6a, and TPC-S2, 6b).** TPC (0.5 g, 1eq, 1.8 mmol) was dissolved in DMF (10 mL) under stirring. **S1** or **S2** (0.5 eq., 0.9 mmol) was dissolved in DMF (5 mL) and EDC (0.5 eq., 0.9 mmol) and HOBt (0.5 eq., mmol) were added followed by stirring for 1 h at 25 °C. The solution of TPC was then added

to the reaction mixture along with sodium bicarbonate ($NaHCO_3$) (0.39 g, 2 eq., 2.16 mmol). The reaction was stirred at 55 °C for 18 h. The reaction mixture was diluted with ice-cold water and dialysed against water for 2 days, ion-exchanged against 10% sodium chloride solution and re-dialysed for 2 days. The purified solution was lyophilized to get a light-yellow solid as the product. **TPC-S1**: yield: 0.63 g (95.5%). $^1$H NMR (500 MHz, $D_2O$): $\delta$ 1.07 (9), 1.26 (5), 1.44 (4), 1.53 (6), 1.97 (N-Ac), 2.30 (3), 2.44–2.61 (8), 2.79 (2), 2.99 [$N(CH_3)_3$], 3.11–3.29 (1,7), 3.67–4.33 (glucose + glucosamine unit), 5.02 (H-1) ppm. **TPC-S2**: yield: 0.71 g (97.3%). $^1$H NMR (500 MHz, $D_2O$): $\delta$ 1.29 (5), 1.51 (4,6), 1.95 (N-Ac), 2.28 (3), 2.77 (2), 2.97 [$N(CH_3)_3$], 3.08 (1), 3.27 (7), 3.67–4.12 (glucose + glucosamine unit), 5.03 (H-1), 7.09 (8), 7.62 (9) ppm.

Note: the numbering of the protons is according to Fig. 1.

**Characterization.** Characterization of the compounds was performed using $^1$H-NMR spectra recorded at 300 K using a Bruker Avance 500 MHz spectrometer. NMR samples were measured in $D_2O$ or DMSO-$d_6$ : $D_2O$ (1 : 1) at a concentration of 10 mg mL$^{-1}$. The final spectra were processed using MestreNova software version 14.2.2-28739. The degree of substitution (DS) for the chitosan conjugates and their precursors was evaluated using the integral values in the $^1$H NMR spectrum and using the equations described below.

$$\text{Degree of mesylation} = \left[\frac{\int \text{CH3}}{\int \text{H2} - \text{H6}} \times \frac{6}{3}\right] \times 100 \quad (1)$$

$$\text{DS for } \mathbf{2}, \mathbf{5} = \left[\frac{\int \text{N-(CH3)3}}{\int \text{H2} - \text{H6}} \times \frac{6}{9}\right] \times 100 \quad (2)$$

$$\text{DS for } \mathbf{3a}, \mathbf{4a}, \mathbf{6a} := \left[\frac{\int (\text{Glucose} - \text{CH3})}{\int \text{H2} - \text{H6(Glucosamine)}} \times \frac{6}{3}\right] \times 100 \quad (3)$$

$$\text{DS for } \mathbf{3b}, \mathbf{4b}, \mathbf{6b} := \left[\frac{\int (\text{Aromatic} - \text{CH}-)}{\int \text{H2} - \text{H6(Glucosamine)}} \times \frac{6}{4}\right] \times 100 \quad (4)$$

### Molecular weight determination

The average molecular weight ($M_w$) and dispersity ($D$) for starting chitosan and its derivatives were assessed by gel permeation chromatography using an Agilent 1260 Infinity Multi-Detector GPC/SEC system (Santa Clara, CA, United States) with the triple detection technique. The measurements were performed using the following modules: Agilent 1260 Infinity Standard Degasser (G1322A), Agilent 1260 Infinity Isocratic Pump (G1310B), Agilent 1260 Infinity Standard Autosampler (G1329B), Agilent 1260 Infinity Thermostated Column Compartment (G1316A), Agilent 1260 Infinity GPC/SEC Multi-Detector Suite (G7800A), Agilent 1260 Infinity MDS RID (G7801A), Agilent 1260 Infinity MDS Viscometer (G7802A) and Agilent 1260 Infinity MDS Light Scattering (G7803A). The column set used for the measurement was 2 × PL aquagel-OH Mixed-H 8 μm and 7.5 × 300 mm (PL1149-6800). Agilent polymethylmethacrylate (PMMA) standards were employed to generate the universal calibration. Chitosan conjugates were dissolved in 0.5 M $NaNO_3$/0.01 M $NaH_2PO_4$ (pH 2) at a concentration of 1 mg mL$^{-1}$ before filtering with a syringe filter of 0.45 μm and 25 mm diameter (Corning® syringe filters). The eluent used was 0.5 M $NaNO_3$/0.01 M $NaH_2PO_4$ (pH 2) and the samples were run with an injection volume of 100 μL and a flow rate of 1 mL min$^{-1}$. Triplicate measurements were done for each sample. Data were processed using Agilent GPC/SEC Multi-Detector software (G7852AA). The $M_w$, $M_n$ and PDI values were determined as calculated by the software.

### Antibacterial assays

**Determination of the minimum inhibitory concentration and minimum bactericidal concentration for *S.* aureus, *E. coli***

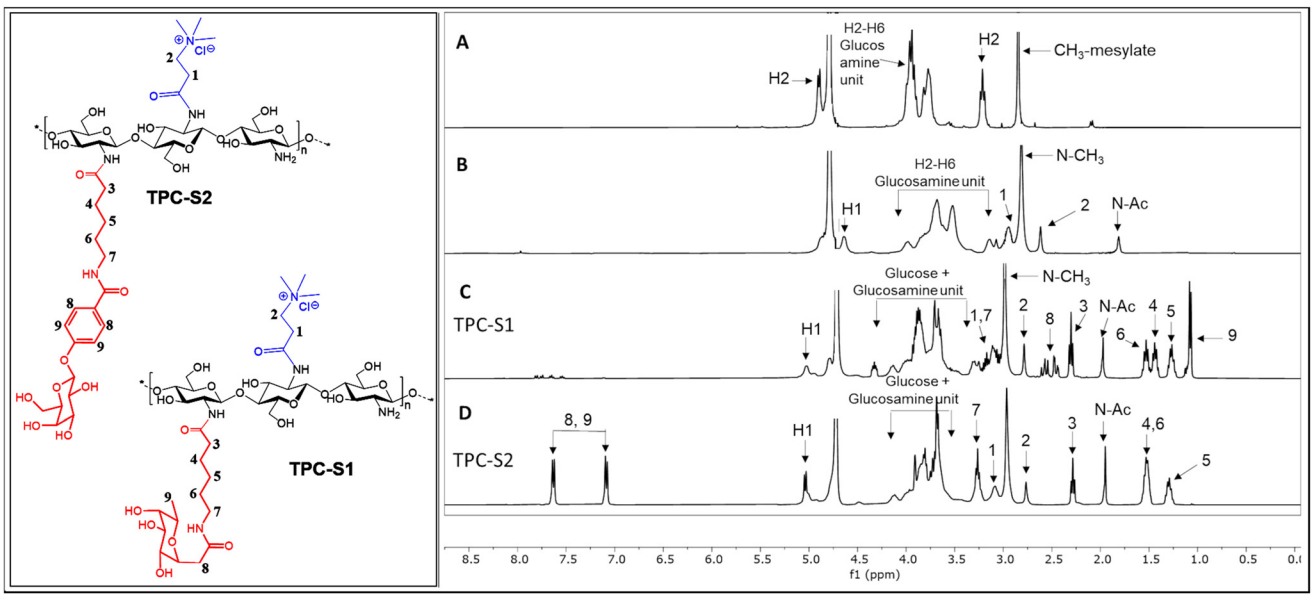


Fig. 1 $^1$H-NMR spectra of (A) chitosan mesylate salt; (B) *N,N,N*-trimethyl *N*-propanoyl-chitosan (TPC); (C) **TPC-S1** conjugate and (D) **TPC-S2** conjugate.

**and *P. aeruginosa*.** The antibacterial assays were performed according to standard CLSI methods for antimicrobial dilution susceptibility tests[20] to measure the minimum inhibitory concentration (MIC) and minimum bactericidal concentration (MBC). The antibacterial activity was tested against Gram positive bacteria *S. aureus* (DSM 20231) and Gram-negative bacteria *E. coli* (ATCC 25922) and *P. aeruginosa* (PA01 DSM19880). The broth microdilution method was used to determine the MIC values in Mueller–Hinton broth (MHB) at pH 7.2. CFU enumeration for MBC assays was performed on blood agar. Chitosan samples were prepared in sterile water at an initial concentration of 32.8 μg $mL^{-1}$, which was serially diluted in MHB by twofold dilution in a 96-well plate. Gentamicin at similar concentrations to chitosan samples was used as the positive control. Overnight cultures were prepared by inoculating each bacterial strain into 20 mL of Brain Heart Infusion Broth (BHI) taken in an Erlenmeyer flask. The flask was then incubated overnight at 37 °C at 180 rpm. A total of three biological replicates were prepared in a similar manner by inoculating individual colonies from each strain. A standard 0.5 McFarland suspension (1–2 × $10^8$ CFU $mL^{-1}$) of the overnight cultures was prepared in MHB and diluted to achieve a final test concentration of 5 × $10^5$ CFU $mL^{-1}$ in the 96-well plate. The plates were then incubated at 35 °C for 18 h before optical density measurement at 600 nm (BioTek PowerWave XS2) to identify wells with bacterial growth. MIC values were determined as the lowest concentrations of the antibacterial agent that completely inhibited growth. For MBC measurements, 2 × 10 μL from each well with no visible growth was placed on blood agar and incubated at 35 °C for 18 h to count the CFU. The MBC was determined as the lowest concentration that achieved a 99.9% decrease in the viable cells.

**Determination of the minimum biofilm eradication concentration for *P. aeruginosa*.** Overnight cultures of *P. aeruginosa* were prepared as described above. The overnight cultures were diluted in BHI to OD = 0.1 using an Ultrospec10 Cell density meter (Amersham Biosciences). The adjusted cultures were added to the wells of three 96-well plates. Peg lids were inoculated by placing them into the wells and incubating at 37 °C in a zip lock bag for 2 h. The peg lids were then transferred into a fresh well plate containing BHI and incubated in a zip lock bag at 37 °C for 24 h. A total of three peg lids with biofilms were prepared in this manner. Treatment with the chitosan–sugar conjugates was performed by transferring the peg lids with the biofilm into well plates (treatment plates) containing serial dilutions of the conjugate solutions in BHI. The peg lids containing the biofilms were then incubated in the treatment plates at 37 °C for 24 h. After incubation, the peg lids were removed from the treatment plate and gently washed by placing them for 1 min in two washing plates, each containing fresh BHI to remove any of the polymers. The peg lids were finally transferred into recovery plates containing TBS and sonicated for 10 min to release the cells from the biofilm to the solution. After sonication, samples were taken out from the wells for CFU enumeration. The peg lids in the recovery plates were then incubated at 37 °C for 72 h; if any viable cells were left in the biofilm, they would result in planktonic growth in the BHI. Planktonic growth in the recovery plate was measured at OD600 at the end of the incubation. The minimal biofilm eradication concentration (MBEC) was the lowest polymer concentration that resulted in the absence of viable cells, even after the resuscitation period.

### Confocal laser scanning microscopy imaging

The antibacterial effect of chitosan derivatives was visualized by LIVE/DEAD staining of *P. aeruginosa* biofilms using the membrane-permeable SYTO 60 and membrane-impermeable TOTO-1 stains and confocal laser scanning microscopy (CLSM). The stain combination was used according to a previously published procedure.[26] Overnight cultures of *P. aeruginosa* (3 biological replicates) were prepared as previously described. The cultures were then adjusted to OD = 0.1 using BHI and 160 μl was transferred to the wells of a 96-well microscopy plate (Ibidi catalogue # 89621) for inoculation at 37 °C for 2 h. The bacterial suspension was then carefully removed by aspiration and replaced with 200 μl of BHI and the plate was incubated at 37 °C for 24 h. After 24 h, the supernatant was replaced with 200 μl of fresh BHI and incubated under similar conditions for another 24 h to allow the biofilm to develop further. Solutions of the chitosan conjugates were prepared in BHI at concentrations equal to 0.025 × MBEC and 0.5 × MBEC. After 48 h of incubation, the supernatant was carefully removed from the wells and replaced with 100 μl of the conjugate solutions, whereas the growth controls were treated with fresh BHI. The microscopy plates were then incubated at 37 °C for 24 h. The supernatant in the wells was then replaced with 180 μl of 0.9% NaCl solution and left for 5 min. The removal and addition of fresh NaCl solution was performed three times. Finally, 100 μl of NaCl solution was added to the wells and known concentrations of SYTO 60 and TOTO1 stains were added to the wells to get final concentrations of 10 μM (SYTO60) and 1 μM (TOTO1) in the wells before imaging.

To determine the interaction of the conjugates with *S. aureus*, a bacterial solution (200 μL) with OD = 0.1 was mixed with BHI containing calcofluor (100 μg $mL^{-1}$) and incubated overnight (37 °C) for growth control. On the other hand, a solution of the conjugate in BHI (150 μL) was incubated with calcofluor (100 μg $mL^{-1}$) in the dark for 4 hours. After this period, 90 μL of the conjugate solution was added to 10 μL of the bacterial solution (OD = 0.1) and incubated overnight (37 °C). For imaging the cells in CLSM, 10 μL of the growth control cells or conjugate-treated cells was placed on a glass slide, left standing for 20 min and washed with de-ionised water (30 μL × 3). The sample was stained with SYTO60 in 0.9% NaCl solution for 20 min in the dark. After washing the sample with de-ionised water (30 μL × 3), a drop of drop protector was applied for 5 min and covered with a second glass slide and visualized under CLSM. Fluorescence was captured with 405 nm excitation and <560 nm emission for calcofluor.

For biofilm visualization, a similar procedure to that described above was followed for preparation.

### Haemolytic activity

Human red blood cell (RBC) concentrate ($6.1 \times 10^{12}$ RBCs $L^{-1}$, total haemoglobin of 208 g $L^{-1}$, and $0.02 \times 10^{9}$ WBCs $L^{-1}$) was used for testing the haemolytic activity of the peptide and the conjugates. RBCs (100 μL) were suspended in tris-buffered saline (TBS; 10 mL; pH = 7.2). The samples were prepared in TBS at an initial concentration of 32 768 μg $mL^{-1}$. 50 μL of the samples at the initial concentration were added to the first two wells of a 96-well plate. The samples were then serially diluted two-fold using TBS to have a minimum concentration of 16 μg $mL^{-1}$. 50 μL of RBC suspension was added to each well and incubated at 37 °C with light shaking for 30 min. Cells treated with TBS and 2% TRITON-X were used as negative and positive controls, respectively. The cell suspensions were centrifuged at 1500 rpm for 10 min, and the supernatant was used for measuring the absorbance of the released haemoglobin at 540 nm with a Thermo Scientific Multiskan Spectrum. The percentage haemolysis was calculated using eqn (5) and the $HC_{50}$ values were reported.

$$\text{Hemolysis rate } (\%) = \frac{A - A_0}{(A_{100} - A_0)} \times 100\% \quad (5)$$

where $A$ is the absorbance of the polymer solutions, $A_0$ is the absorbance of the negative control, and $A_{100}$ is the absorbance of the positive control.

## Results and discussion

Multivalent display of carbohydrate epitopes plays a pivotal role in the engagement of the immune machinery. To couple aryl-*O*-galactoside and *C*-fucoside epitopes onto chitosan backbone amine groups, prior derivatization with a suitable linker was required.

### Synthesis of *C*-fucosyl and aryl-*O*-galactosyl building blocks

2-(Tri-*O*-acetyl-α-L-fucopyranosyl) acetic acid (**S5**) was prepared from commercial L-fucose as described[21] (see Scheme 1). EDAC/HOBt-mediated coupling of the 6-(benzyloxy)-6-oxohexan-1-aminium *p*-toluenesulphonate linker in the presence of NMM and DMF as solvent resulted in the isolation of the **S1** precursor, protected as benzyl ester, in 75% yield (**S4**). Catalytic hydrogenation with Pd/C in THF/$H_2O$ and subsequent deacetylation carried out with LiOH in THF/$H_2O$ afforded **S1** as a white solid in a quantitative yield.

Starting from galactose pentaacetate, 4-(tetra-*O*-acetyl-β-D-galactopyranosyloxy) benzoic acid (**S8**) was easily isolated as previously reported[22] (see Scheme 1). Conversion into galactosyl derivative **S2** was achieved under the same conditions described for **S1**. Amide-coupling with the 6-(benzyloxy)-6-oxohexan-1-aminium *p*-toluenesulphonate linker resulted in 59% yield, followed by final deprotection steps affording the desired product **S2** in 92% yield.

### Synthesis of chitosan–sugar conjugates

To link the glycosidic moieties to the chitosan backbone, we performed amide coupling at the amino group of chitosan using the free carboxylic acids of the glycosides **S1** and **S2**. Chemical modification on native chitosan is very difficult owing to its poor aqueous solubility and non-solubility in most organic solvents. Hence, previous studies reported several synthetic strategies such as using protective groups at either one or two of the free –OH groups.[23–25] Protected chitosan is then soluble in some organic solvents and hence reactions can be performed in a homogeneous medium for *N*-modifications with high DS (up to 100%) in the products.[25,26] However, introduction and removal of protective groups increases the number of synthetic steps and it results in significant trimming of the polymer chain.[27]

Hence, our study was aimed at introducing low DS glycosides on the chitosan backbone. For this purpose, we optimized a direct synthetic method avoiding the use of protection group. To overcome the solubility issue of chitosan, we prepared the mesylate salt of chitosan, which has excellent aqueous solubility and high solubility in polar organic solvents such as DMF and DMSO. By using the mesylate salt of chitosan, we initially modified the amino group of chitosan to include two cationic groups, namely, the trimethyl amino group and the *N,N,N*-trimethyl-*N*′-propanoyl group. For **TMC**, chitosan was treated with methyl iodide/$Cs_2CO_3$ in DMSO, and using calculated equivalents of methyl iodide (MeI) we obtained a DS = 25%. The second chitosan derivative, **TPC**, was synthesized in two steps: first *N*-acylation using 3-bromopropanoic acid and then substituting the bromide with the trimethylamino group. The two cationic chitosan derivatives **2** and **5** having a DS of 25% were synthesized as shown in Scheme 1. The purpose of introducing the cationic trimethylamino group on chitosan is for taking advantage of its high aqueous solubility and broad-spectrum antimicrobial properties as observed in previous studies.[19,27] We then designed a series of chitosan–sugar conjugates with the aim of having 25–30% of **S1** and **S2** glycosides grafted on native chitosan as well as on modified chitosan, **2** and **5**. We achieved this by reacting the carboxylic residue of **S1** and **S2** with the free amino group of either native chitosan or the two cationic chitosan derivatives by using EDC/HOBt coupling. Initially, several optimization reactions for the amide coupling reaction were performed as shown in the ESI.† The best results were eventually obtained with EDC/HOBt as coupling reagents in the presence of $NaHCO_3$ and in DMF as solvent. By using 0.5 equivalents of **S1** and **S2** in the reaction media, we obtained a DS of 25–27% for the desired conjugates (Scheme 1).

Previous studies reported coupling of arginine to chitosan by using EDC/NHS in acetic acid resulting in only 17% DS using an excess of reagent.[28] Similar conditions were used for histidine–chitosan linkage resulting in 29% DS using an excess of reagent.[29] Our method utilizing the mesylate salt of chitosan provides a more efficient synthetic method. The main advantages of the method are reproducible DS (~25%)

Table 1 Physico-chemical properties of the synthesized conjugates

| Compd no. | Conjugate | Degree of substitution | | | $M_w$ (Da) | $M_n$ (Da) | $D$ |
|---|---|---|---|---|---|---|---|
| | | Cationic group (%) | Sugar (%) | Free amine (%) | | | |
| **3a** | CS-S1 | 0 | **S1** (25) | 75 | 8187 | 4947 | 1.65 |
| **3b** | CS-S2 | 0 | **S2** (25) | 75 | 7680 | 7486 | 1.02 |
| **4a** | TMC-S1 | TMC (25) | **S1** (27) | 48 | 7880 | 6638 | 1.18 |
| **4b** | TMC-S2 | TMC (25) | **S2** (27) | 48 | 7148 | 439 | 1.11 |
| **6a** | TPC-S1 | TPC (25) | **S1** (27) | 48 | 7878 | 5715 | 1.37 |
| **6b** | TPC-S2 | TPC (25) | **S2** (27) | 48 | 8149 | 6509 | 1.25 |

$M_w$ = weight average molecular weight; $M_n$ = number average molecular weight; $D$ = dispersity.

obtained with only half equivalent of the reagent, applicable for reactions with different functional moieties and reactions in homogeneous organic media. As seen in Table 1, we have a higher ratio of free amino groups in CS-S1/S2 (75%) than that in TMC-S1/S2 (48%) and TPC-S1/S2 (48%). Since the trimethyl amino group in chitosan has previously shown high antibacterial activity and improved aqueous solubility,[25] the aim of this study was also to observe any synergistic effect of the sugar and the cationic group on the antibacterial activity of the conjugates. Table 1 also shows the weight average molecular weight ($M_w$) and dispersity of the conjugates as determined by GPC. We observe that despite a reduction in the $M_w$ of the conjugates from the original chitosan due to the synthetic modification, we have a uniform $M_w$ distribution for all the conjugates. The similar $M_w$ values obtained after the synthetic modification also validate the reproducibility of the synthetic procedure using the chitosan mesylate salt. The $M_w$ values for the conjugates are in the range of 7.1–8.1 kDa and the dispersity lies between 1.0 and 1.6 for all the conjugates. A great advantage of introducing the cationic group and **S1**/**S2** onto the chitosan backbone is that they convert an insoluble biopolymer into a modified polymer exhibiting significantly enhanced aqueous solubility, which is a pre-requisite for biological studies.

We characterized the conjugates by $^1$H-NMR spectroscopy. Fig. 1 shows the comparison of the $^1$H-NMR spectra of the chitosan mesylate salt, TPC, TPC-S1 and TPC-S2. Compared to spectrum A, B shows the presence of two new peaks for protons 1 and 2. Additionally, the appearance of the N-$(CH_3)_3$ peak at 2.81 ppm further confirms the attachment of the *N*,*N*,*N*-trimethylamino propanoyl group to chitosan. Spectra C and D represent TPC-S1 and TPC-S2. In spectrum C for TPC-S1, several new peaks appear in the region of 1.07 to 2.61 ppm, which correspond to protons from the linkers in the sugar (see the ESI†). Moreover, additional peaks from the glucose unit are seen merged with the protons of the glucosamine unit of chitosan. Similarly, for TPC-S2 in spectrum D, we see new peaks from 1.29 to 2.28 ppm and peaks from the glucose unit merge with the glucosamine unit of chitosan. Furthermore, the conjugation of **S2** can be confirmed by the appearance of the protons in the aromatic region at 7.08 and 7.62 ppm corresponding to the benzene ring of the aryl moiety. Similarly, the conjugation of **S1** and **S2** with chitosan and TMC was confirmed from their respective $^1$H-NMR spectra. All spectra for intermediates and conjugates are provided in the ESI.† The DS for the chitosan derivatives and the chitosan–sugar conjugates was calculated from the integrals in the $^1$H-NMR spectra using the equations in the Experimental section and the results are given in Table 1.

### Antibacterial properties of chitosan–sugar conjugates

We initially screened the series of six conjugates against three bacterial strains – *S. aureus*, *E. coli* and *P. aeruginosa*. The results are reported as the Minimum Inhibitory Concentration (MIC) and Minimum Bactericidal Concentration (MBC) (Table 2). The conjugates in general displayed higher activity toward Gram positive *S. aureus* than towards the two Gram negative strains. Of the two Gram negative bacterial strains, *P. aeruginosa* was more susceptible to the conjugates. As seen in Table 2, **TMC-S1** (**4a**) and **TMC-S2** (**4b**) are the most active of the six conjugates toward *P. aeruginosa* with an MIC of 256 μg $mL^{-1}$. Conjugates **4a**, **4b**, **6a** and **6b** displayed high activity toward *S. aureus* (MIC = 64–128 μg $mL^{-1}$). All the conjugates remained moderately active toward the Gram negative *E. coli*. Conjugates **CS-S1** and **CS-S2** remained low in activity and this difference can be justified by the absence of the cationic trimethylamino group unlike the remaining four conjugates. We observed that the presence of the cationic group increases the inhibitory effect of the conjugates by 1–3 fold. These results are consistent with the previously reported studies where chitosan modified with cationic groups such as trimethylammoniumyl and guanidinyl showed enhanced antimicrobial activity toward Gram positive and Gram-negative bacteria compared to native chitosan.[10,19,26,30] We further confirmed the accuracy of the inhibitory concentration of the conjugates by determining their minimum bactericidal concentration values. As seen in Table 2, the MBC values are within 1–2 fold dilution of the MIC values of the conjugates. Thus, all the six conjugates showed bactericidal property toward the three tested strains.

To assess the preliminary toxicity of the conjugates, we tested them against human red blood cells (RBCs). We determined the lowest concentrations corresponding to haemolysis of the RBCs and calculated the $HC_{50}$ and $HC_5$ values (Table 2). The conjugates showed non-haemolytic properties. As seen in Table 2, CS-S1 and CS-S2 did not show a haemolytic effect with

**Table 2** Table showing the antibacterial activity and selectivity toward bacterial strains in the planktonic form

| | *S. aureus* | | *E. coli* | | *P. aeruginosa* | | | | Selectivity HC50/MIC | | |
|---|---|---|---|---|---|---|---|---|---|---|---|
| Conjugate | MIC (μg ml$^{-1}$) | MBC (μg ml$^{-1}$) | MIC (μg ml$^{-1}$) | MBC (μg ml$^{-1}$) | MIC (μg ml$^{-1}$) | MBC (μg ml$^{-1}$) | HC50 (μg ml$^{-1}$) | HC5 (μg ml$^{-1}$) | *S. aureus* | *E. coli* | *P. aeruginosa* |
| CS-S1 (**3a**) | 512 | 1024 | 2048 | 2048 | 1024 | 1024 | ≥32 768 | 1024 | ≥32 | ≥16 | ≥32 |
| CS-S2 (**3b**) | 256 | 256 | 2048 | 4096 | 512 | 1024 | ≥32 768 | 1024 | ≥64 | ≥16 | ≥64 |
| TMC-S1 (**4a**) | 128 | 256 | 1024 | 2048 | 256 | 256 | 16 384 | 512 | 64 | 64 | 64 |
| TMC-S2 (**4b**) | 64 | 128 | 2048 | 2048 | 256 | 512 | 16 384 | 512 | 64 | 8 | 64 |
| TPC-S1 (**6a**) | 128 | 128 | 1024 | 2048 | 512 | 1024 | 16 384 | 512 | 32 | 16 | 32 |
| TPC-S2 (**6b**) | 128 | 256 | 512 | 1024 | 512 | 1024 | 16 384 | 256 | 32 | 32 | 32 |

MIC = minimum inhibitory concentration; MBC = minimum bactericidal concentration; $HC_{50}$ and $HC_5$ = concentrations causing 50% and 5% haemolysis in red blood cells, respectively.

$HC_{50}$ values of ≥32 768 μg mL$^{-1}$, while all the remaining four conjugates displayed a very low toxicity of 16 384 μg mL$^{-1}$. The $HC_5$ values for the chitosan–sugar conjugates showed that the toxicity of unmodified chitosan was lower than that of chitosan modified with cationic derivatives. The haemolysis (%) of RBCs caused by the conjugates against the measured concentrations is shown in Fig. 2. In general, a lower toxicity of the conjugates is expected where a non-toxic polymer (chitosan) is combined with a low toxicity sugar molecule. These results are consistent with previous studies where the combination of chitosan even with toxic antimicrobials such as antimicrobial peptides, ciprofloxacin, and colistin resulted in significant overall lowering of toxicity of the conjugates.[13,31,32] The lower haemolytic activity gave higher selectivity of the conjugates towards all the bacterial strains in the planktonic state (Table 2).

To determine if the conjugates would be effective in eradicating *P. aeruginosa* biofilms, we tested all the conjugates within a similar concentration range and assessed the Minimum Biofilm Eradication Concentration (MBEC). As reported in Table 3, **TMC-S1**, **TMC-S2** and **TPC-S2** were highly effective in eradicating *P. aeruginosa* biofilms with MBEC values of 8–16 μg mL$^{-1}$. Conversely, these three conjugates displayed moderate activity towards *P. aeruginosa* in the planktonic form. **CS-S2** and **TPC-S1** conjugates also showed high activity toward biofilms with a MBEC of 64 μg mL$^{-1}$. The least active of all the conjugates was **CS-S1**. Since the DS of the sugar moieties is similar in all the conjugates, the MBEC values give us a comparative analysis of the activity of the conjugates against biofilms. Table 3 shows that each series of conjugates (containing **S1** and **S2** glycosides) displayed similar antibacterial activity toward *P. aeruginosa* with no difference in their MIC values. However, a clear difference in the antibiofilm activity of the conjugates is observed. All conjugates containing the **S2** glycoside (**CS-S2**, **TMC-S2** and **TPC-S2**) were more effective in eradicating *P. aeruginosa* biofilms. Significant difference is observed within the CS conjugates where the MBEC of **CS-S1** is 4 times that of **CS-S2**. On the other hand, the MBEC values of **TMC-S2** and **TPC-S2** conjugates varied only by 2-fold compared to their **S1** counterparts. Thus, considering the antibiofilm activity toward *P. aeruginosa*, we can conclude

**Table 3** Table showing the comparison of the activity/selectivity of the conjugates against *P. aeruginosa* in the planktonic form and biofilms

| | Antibacterial activity | | Selectivity | |
|---|---|---|---|---|
| Conjugate | Planktonic MIC (μg ml$^{-1}$) | Biofilm MBEC (μg ml$^{-1}$) | Planktonic $HC_{50}$/MIC | Biofilm $HC_{50}$/MBEC |
| CS-S1 (**3a**) | 1024 | 256 | ≥32 | ≥128 |
| CS-S2 (**3b**) | 512 | 64 | ≥64 | ≥512 |
| TMC-S1 (**4a**) | 256 | 16 | 64 | 1024 |
| TMC-S2 (**4b**) | 256 | 8 | 64 | 2048 |
| TPC-S1 (**6a**) | 512 | 32 | 32 | 512 |
| TPC-S2 (**6b**) | 512 | 16 | 32 | 1024 |

MIC = minimum inhibitory concentration; MBEC = minimum biofilm eradication concentration; $HC_{50}$ = concentration causing 50% haemolysis in red blood cells,.

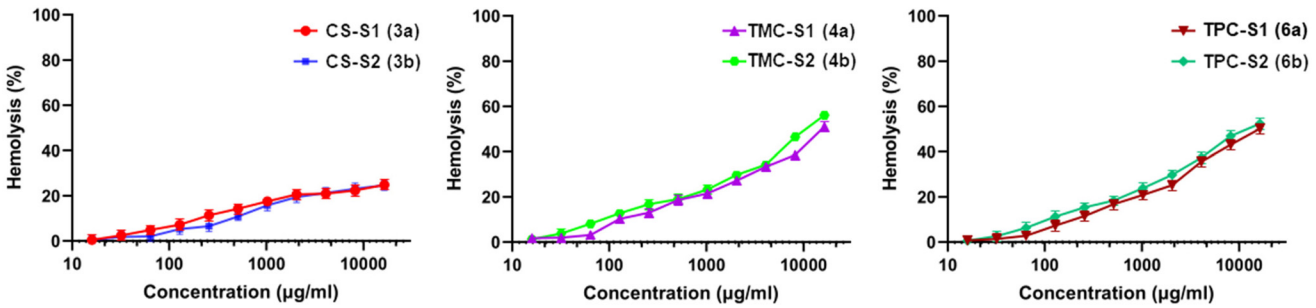


**Fig. 2** Graphs showing the hemolytic activity (%) against concentration of the chitosan–sugar conjugates.

that the *O*-galactoside **S2** conjugates were more efficient than the *C*-fucoside **S1** conjugates. Few studies reported the capability of chitosan and its conjugates to inhibit biofilms. Conjugates of chitosan with the aminoglycoside antibiotic streptomycin were capable of disrupting the biofilms formed only by Gram positive bacteria but not by Gram negative bacteria such as *P. aeruginosa.*[17] Chitosan derivatives containing different combinations of cationic and hydrophobic groups were also highly effective in eradicating the biofilm population of *Staphylococcus aureus.*[33] Biofilm inhibition up to 50–70% was achieved for *P. aeruginosa* using chitosan stabilized silver and gold nanoparticles,[34] while chitosan itself was capable of inhibiting biofilms of several Gram positive bacteria.[35,36] However, no study with chitosan conjugates for complete eradication of *P. aeruginosa* biofilms has been reported so far. *P. aeruginosa* biofilms possess high levels of intrinsic antibiotic tolerance and hence cannot be eradicated using the available antibiotics. Our study has shown that by using saccharidic ligands for LecA and LecB to decorate chitosan, we have been able to develop conjugates that effectively disrupt pre-formed *P. aeruginosa* biofilms.

The higher antibiofilm activity of **TMC-S1/S2** and **TPC-S1/S2** than that of **CS-S1/S2** conjugates reveals that the presence of the cationic trimethyl amino group contributes positively to the antibiofilm activity. Although, **CS-S1/S2** conjugates disrupted the pre-formed *P. aeruginosa* biofilms, higher antibiofilm activity was observed when the sugar moieties were combined with the trimethylamino groups. This demonstrates the synergistic effect of the two functionalities against *P. aeruginosa* biofilms. Furthermore, **TMC-S1/S2** showed improved activity compared to **TPC-S1/S2** conjugates. This indicates that the cationic group that is close to the polymer chain increases the activity, as was also observed in a previous study.[27] As seen in Table 3, the selectivity of the conjugates toward *P. aeruginosa* biofilms is significantly higher than the selectivity toward individual cells.

The MBEC assay identifies the concentration required to kill the last cell in the biofilm. However, antimicrobial compounds might kill most of the bacteria in the biofilm at much lower concentrations. We therefore enumerated the number of viable cells in the biofilms after 24 h treatment with the conjugates at concentrations corresponding to the highest, intermediate and the lowest dilutions used for the MBEC measurement. The graphs in Fig. 3 show the viability of the biofilm population of *P. aeruginosa* after treatment with different concentrations of the conjugates and for the growth control. Results show that **CS-S1**, **CS-S2**, **TMC-S1** and **TMC-S2** can reduce the biofilm population by 50% (3.5 log difference) at 2–4× dilution of their MBECs, while **TPC-S1** and **TPC-S2** reduced the bacterial population by 3 log difference at 4–8× dilutions of their MBECs.

The antibacterial effect of conjugates was visualized by live/dead staining of *P. aeruginosa* biofilms using a confocal laser scanning microscope (CLSM). We used a combination of the membrane-permeable SYTO 60 and membrane-impermeable TOTO-1 stains for staining the cells in the biofilm. The red

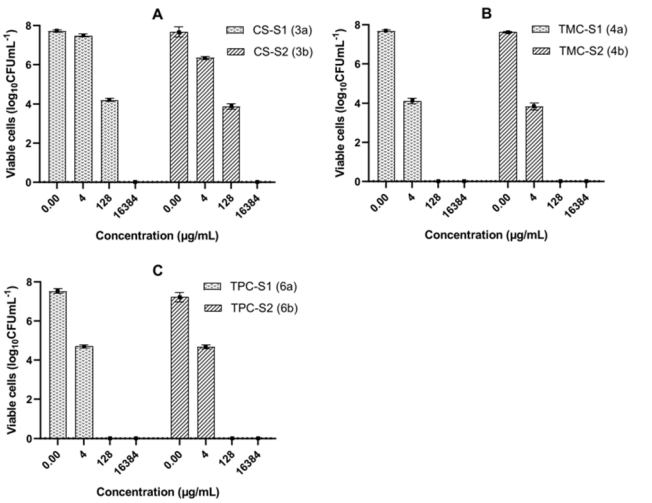


**Fig. 3** Graphs showing the viability of the biofilm population of *P. aeruginosa* when treated with different concentrations of (A) **CS-S1** and **CS-S2**; (B) **TMC-S1** and **TMC-S2**; (C) **TPC-S1** and **TPC-S2** conjugates. Each bar in the graphs represents the mean of three biological replicates and the error bars represent the standard deviation.

colour in the images represents live cells while the green colour represents dead cells. Fig. 4 shows the images of *P. aeruginosa* biofilms treated with the two highly active conjugates **TMC-S1** and **TMC-S2.** The untreated biofilm 1 is uniform in structure containing viable cells (red color). The biofilm treated with a low concentration (0.025 × MBEC) of the conjugate **TMC-S1** (0.4 μg $mL^{-1}$) shows dead cells (green color) scattered over the biofilm (image 2), whereas the biofilm treated with a higher concentration (0.5 × MBEC) of **TMC-S1** (8 μg $mL^{-1}$) contains mostly dead cells (image 3). A similar effect is seen for biofilms (images 4 and 5) treated with low and high concentrations (0.2 μg $mL^{-1}$ and 4 μg $mL^{-1}$) of **TMC-S2.**

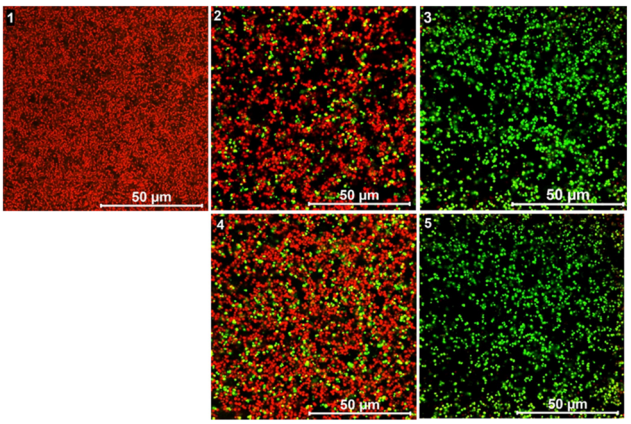


**Fig. 4** 2D confocal images of the biofilm population of *P. aeruginosa* where red = live cells and green = dead cells. (1) Growth control; (2) biofilm treated with 0.025 × MBEC of **TMC-S1**; (3) biofilm treated with 0.5 × MBEC of **TMC-S1**; (4) biofilm treated with 0.025 × MBEC of **TMC-S2** and (5) biofilm treated with 0.5 × MBEC of **TMC-S2**.

Hence, the CLSM imaging of treated and untreated biofilms confirmed the strong effect that these conjugates have on biofilm viability.

To confirm the ability of conjugates to penetrate *P. aeruginosa* biofilms, we performed 3D imaging of **TMC-S2**-treated biofilms compared to the growth control (Fig. 5). Image 1 shows that the biofilm of the growth control has a thickness of 12.3 μm. When the biofilm was treated with a lower concentration (0.025 × MBEC) of **TMC-S2** (image 2), we observed an accumulation of dead cells throughout the biofilm and the thickness of the biofilm was reduced to 6.1 μm. At a higher concentration (0.5 × MBEC), the biofilm (image 3) mostly shows dead cells, with a significantly reduced thickness of 3 μm. Image 3 also confirms that the dead cells are not only present on the surface but also in the deeper layers of the biofilm, suggesting that the conjugates are capable of dispersing into the biofilm matrix.

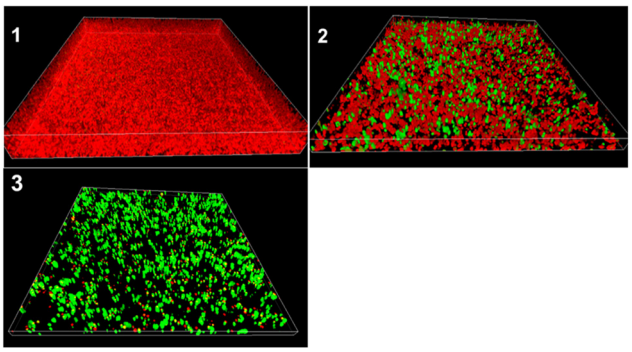


**Fig. 5** 3D confocal images of the biofilm population of *P. aeruginosa* where red = live cells and green = dead cells. (1) Growth control, (2) biofilm treated with 0.025 × MBEC of **TMC-S2** and (3) biofilm treated with 0.5 × MBEC of **TMC-S2**.

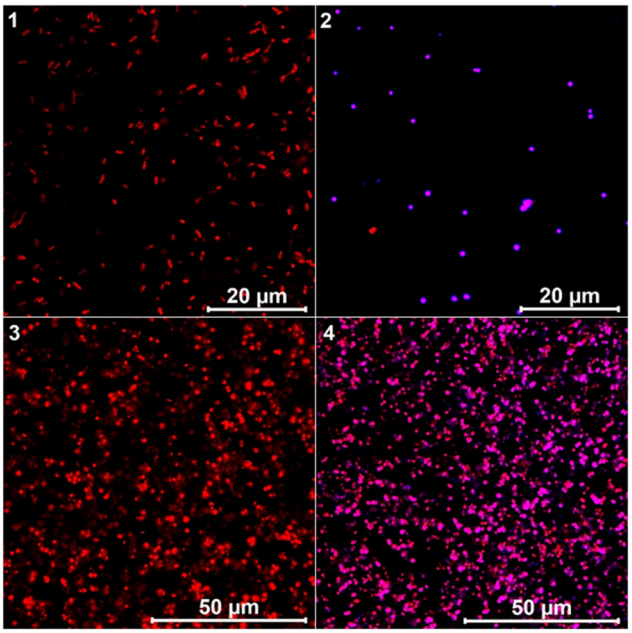


**Fig. 6** 2D confocal images showing *P. aeruginosa* where red = bacterial cells stained with calcofluor and SYTO60; blue = TMC-S2 stained with calcofluor; pink = overlapping of **TMC-S2** with *P. aeruginosa* suggesting binding. (1) Growth control (planktonic form); (2) cells treated with 0.025 × MBEC of **TMC-S2**-calcofluor, (3) growth control (biofilm) and (4) biofilm treated with 0.025 × MBEC of **TMC-S2**-calcofluor.

To confirm that the conjugates interact with *P. aeruginosa*, we visualized the effect of the conjugate **TMC-S2** on *P. aeruginosa* cells by fluorescence staining and confocal microscopy. Calcofluor which binds to chitosan[37] was used as a fluorescent probe to visualize the conjugate **TMC-S2**. The bacterial cells were treated either with calcofluor (for growth control) or **TMC-S2**-calcofluor and stained with SYTO60 to visualize the cells. Fig. 6 shows the 2D CLSM images of individual *P. aeruginosa* cells untreated and treated with **TMC-S2**-calcofluor. As seen, the growth control (image 1) contains viable cells (red) while the cells treated with **TMC-S2**-calcofluor emit pink fluorescence (image 2). Images 3 and 4 show similar observations when biofilms of *P. aeruginosa* are untreated and treated with **TMC-S2**-calcofluor. These images confirm that **TMC-S2** can interact with *P. aeruginosa* cells both in the planktonic form and in the biofilm.

## Conclusions

Development of novel antimicrobials that are based on biocompatible materials and can operate by a different mode of action to target bacterial biofilms, such as those formed by *P. aeruginosa*, is a promising avenue to address the problem of antibiotic resistance. However, the design and development of bio-based materials endowed with high efficiency against bacteria is often very challenging. In this study, we report the synthesis of a series of novel chitosan–sugar conjugates by direct chemical modification of the chitosan backbone. The synthetic method we developed gave excellent yield and reproducibility. We observed that by attaching either sugar moieties or a combination of sugar and cationic moieties on chitosan the bactericidal effect is enhanced, on both Gram-positive and Gram-negative bacteria. More importantly, we showed that the series of conjugates developed were highly effective in eradicating the biofilm population of *P. aeruginosa*. Furthermore, these conjugates displayed very low toxicity and hence were highly selective toward *P. aeruginosa*. Structure–activity relationship analyses revealed that the conjugates containing a combination of sugar (aryl-*O*-galactoside or *C*-fucoside) and cationic moieties on chitosan were the most efficient in disrupting the biofilms. We confirmed this by CLSM imaging of the dead cells present in conjugate-treated *P. aeruginosa* biofilms. 3D imaging showed that the conjugates were capable of dispersing into the biofilm matrix which resulted in a significant reduction in the thickness of the biofilm. By using fluorescence staining and CLSM imaging, we showed that the conjugates do interact with individual bacterial cells in the biofilm.

## Author contributions

P.S.: conceptualization, investigation, formal analysis, methodology, visualization, writing – original draft; F.P.: synthesis of glycans, writing; K.L.M.: synthesis of sugars; O.E.S.: investigation, formal analysis, writing – review and editing; R.L.M.: conceptualization, writing – review and editing, supervision, project administration, funding acquisition; C.N.: conceptualization, writing – review and editing, supervision, project administration, funding acquisition.

## Conflicts of interest

There are no conflicts to declare.

## Acknowledgements

The research work was supported by MUR, Italy (PRIN22 20222BLNZS). We acknowledge the additional support from Erasmus grant, University of Iceland. This manuscript is based upon the work from COST Action Functional Glyconanomaterials for the Development of Diagnostics and Targeted Therapeutic Probes (GLYCONanoPROBES) CA18132 supported by COST (European Cooperation in Science and Technology).

## References

1 W. H. Organization, *Prioritization of pathogens to guide discovery, research and development of new antibiotics for drug-resistant bacterial infections, including tuberculosis, Report 9240026436*, World Health Organization, 2017.
2 C. J. Murray, K. S. Ikuta, F. Sharara, L. Swetschinski, G. R. Aguilar, A. Gray, C. Han, C. Bisignano, P. Rao and E. Wool, *Lancet*, 2022, **399**, 629–655.
3 M. G. Wilson and S. Pandey, Pseudomonas aeruginosa. [Updated 2023 Aug 8]. In *StatPearls* [Internet], StatPearls Publishing, Treasure Island (FL), 2024. Available from: **https://www.ncbi.nlm.nih.gov/books/NBK557831/**.
4 Z. Pang, R. Raudonis, B. R. Glick, T. J. Lin and Z. Cheng, *Biotechnol. Adv.*, 2019, **37**, 177–192.
5 P. S. Stewart and J. W. Costerton, *Lancet*, 2001, **358**, 135–138.
6 M. C. Walters 3rd, F. Roe, A. Bugnicourt, M. J. Franklin and P. S. Stewart, *Antimicrob. Agents Chemother.*, 2003, **47**, 317–323.
7 G. Michaud, R. Visini, M. Bergmann, G. Salerno, R. Bosco, E. Gillon, B. Richichi, C. Nativi, A. Imberty, A. Stocker, T. Darbre and J.-L. Reymond, *Chem. Sci.*, 2016, **7**, 166–182.
8 D. Boffoli, F. Bellato, G. Avancini, P. Gurnani, G. Yilmaz, M. Romero, S. Robertson, F. Moret, F. Sandrelli, P. Caliceti, S. Salmaso, M. Cámara, G. Mantovani and F. Mastrotto, *Drug Delivery Transl. Res.*, 2022, **12**, 1788–1810.
9 I. Aranaz, A. R. Alcántara, M. C. Civera, C. Arias, B. Elorza, A. Heras Caballero and N. Acosta, *Polymers*, 2021, **13**, 3256.
10 P. Sahariah and M. Másson, *Biomacromolecules*, 2017, **18**, 3846–3868.
11 Y. Qin and P. Li, *Int. J. Mol. Sci.*, 2020, **21**, 499.
12 M. E. Abd El-Hack, M. T. El-Saadony, M. E. Shafi, N. M. Zabermawi, M. Arif, G. E. Batiha, A. F. Khafaga, Y. M. Abd El-Hakim and A. A. Al-Sagheer, *Int. J. Biol. Macromol.*, 2020, **164**, 2726–2744.
13 P. Sahariah, K. K. Sørensen, M. Á. Hjálmarsdóttir, Ó. E. Sigurjónsson, K. J. Jensen, M. Másson and M. B. Thygesen, *Chem. Commun.*, 2015, **51**, 11611–11614.
14 C. Liang, F. Yuan, F. Liu, Y. Wang and Y. Gao, *Int. J. Biol. Macromol.*, 2014, **70**, 427–434.
15 T. Mohan, K. S. Kleinschek and R. Kargl, *Carbohydr. Polym.*, 2022, **280**, 118875.
16 D. Pranantyo, L. Q. Xu, E. T. Kang and M. B. Chan-Park, *Biomacromolecules*, 2018, **19**, 2156–2165.
17 A. Zhang, H. Mu, W. Zhang, G. Cui, J. Zhu and J. Duan, *Sci. Rep.*, 2013, **3**, 3364.
18 R. Pakkulnan, N. Thonglao and S. Chareonsudjai, *Sci. Rep.*, 2023, **13**, 1059.
19 P. Sahariah, G.-I. Kontogianni, E. Scoulica, O. E. Sigurjonsson and M. Chatzinikolaidou, *Carbohydr. Polym.*, 2023, **312**, 120796.
20 F. R. Cockerill, *Methods for Dilution Antimicrobial Susceptibility Tests for Bacteria That Grow Aerobically*, Approved Standard, Ninth Edition, M07-A9 Vol. 32 No. 2, 2012.
21 E. M. Johansson, S. A. Crusz, E. Kolomiets, L. Buts, R. U. Kadam, M. Cacciarini, K. M. Bartels, S. P. Diggle, M. Cámara, P. Williams, R. Loris, C. Nativi, F. Rosenau, K. E. Jaeger, T. Darbre and J. L. Reymond, *Chem. Biol.*, 2008, **15**, 1249–1257.
22 R. U. Kadam, M. Bergmann, M. Hurley, D. Garg, M. Cacciarini, M. A. Swiderska, C. Nativi, M. Sattler, A. R. Smyth, P. Williams, M. Cámara, A. Stocker, T. Darbre and J.-L. Reymond, *Angew. Chem., Int. Ed.*, 2011, **50**, 10631–10635.
23 K. Kurita, H. Ikeda, M. Shimojoh and J. Yang, *Polym. J.*, 2007, **39**, 945–952.
24 O. V. Rúnarsson, C. Malainer, J. Holappa, S. T. Sigurdsson and M. Másson, *Carbohydr. Res.*, 2008, **343**, 2576–2582.
25 B. E. Benediktsdóttir, V. S. Gaware, Ö. V. Rúnarsson, S. Jónsdóttir, K. J. Jensen and M. Másson, *Carbohydr. Polym.*, 2011, **86**, 1451–1460.
26 P. Sahariah, B. M. Óskarsson, M. Á. Hjálmarsdóttir and M. Másson, *Carbohydr. Polym.*, 2015, **127**, 407–417.
27 P. Sahariah, V. S. Gaware, R. Lieder, S. Jónsdóttir, M. Á. Hjálmarsdóttir, O. E. Sigurjonsson and M. Másson, *Mar. Drugs*, 2014, **12**, 4635–4658.
28 B. P. Antunes, A. F. Moreira, V. M. Gaspar and I. J. Correia, *Carbohydr. Polym.*, 2015, **130**, 104–112.
29 V. M. Gaspar, J. G. Marques, F. Sousa, R. O. Louro, J. A. Queiroz and I. J. Correia, *Nanotechnology*, 2013, **24**, 275101.
30 D. Yan, Y. Li, Y. Liu, N. Li, X. Zhang and C. Yan, *Molecules*, 2021, **26**, 7136.

31 A. R. Egorov, M. N. Kurasova, O. Khubiev, N. A. Bogdanov, A. G. Tskhovrebov, A. A. Kirichuk, V. N. Khrustalev, V. V. Rubanik, V. V. Rubanik and A. S. Kritchenkov, *Mendeleev Commun.*, 2022, **32**, 774–776.
32 N. V. Dubashynskaya, A. N. Bokatyi, A. V. Dobrodumov, I. V. Kudryavtsev, A. S. Trulioff, A. A. Rubinstein, A. D. Aquino, Y. A. Dubrovskii, E. S. Knyazeva, E. V. Demyanova, Y. A. Nashchekina and Y. A. Skorik, *Int. J. Mol. Sci.*, 2023, **24**, 166.
33 P. Sahariah, M. Másson and R. L. Meyer, *Biomacromolecules*, 2018, **19**, 3649–3658.
34 M. F. Ma, F. Y. Faris Taufeq, S. Suleman Ismail Abdalla and H. Katas, *RSC Adv.*, 2022, **12**, 19297–19312.
35 B. Orgaz, M. M. Lobete, C. H. Puga and C. San Jose, *Int. J. Mol. Sci.*, 2011, **12**, 817–828.
36 V. Felipe, M. L. Breser, L. P. Bohl, E. Rodrigues da Silva, C. A. Morgante, S. G. Correa and C. Porporatto, *Int. J. Biol. Macromol.*, 2019, **126**, 60–67.
37 C. A. Marangon, V. C. A. Martins, M. H. Ling, C. C. Melo, A. M. G. Plepis, R. L. Meyer and M. Nitschke, *ACS Appl. Mater. Interfaces*, 2020, **12**, 5488–5499.